第27卷第6期　　热　能　动　力　工　程　　Vol. 27,No. 6
2012年11月　　JOURNAL OF ENGINEERING FOR THERMAL ENERGY AND POWER　　Nov. ,2012

文章编号:1001 - 2060(2012)06 - 0721 - 05

基于递归模糊神经网络的PEMFC温度控制研究

李春华^1,朱新坚^2
(1. 江苏科技大学 电子信息学院,江苏 镇江 212003;2. 上海交通大学 燃料电池研究所,上海 200240)

摘　要:质子交换膜燃料电池(PEMFC)的工作温度对其发电性能和电池寿命具有重要影响,但由于PEMFC的非线性和时变特性,传统的控制策略较难获得很好的温度控制性能,以此推荐使用一种具有模糊推理、在线学习和动态映射能力的递归模糊神经网络控制器(RFNNC),将PEMFC工作温度有效控制在允许范围内。基于能量守恒定律建立PEMFC的动态热模型,采用误差反传技术对该控制器参数进行自适应调整。仿真实验显示,RFNNC仅需35 s达到稳态,波动较小,比较RFNNC与PI控制和模糊控制的控制结果表明,推荐使用的RFNNC具有较好的温度跟踪性能。

关　键　词:质子交换膜燃料电池(PEMFC);热模型;递归模糊神经网络(RFNN);温度控制

中图分类号:TM91;TK91　　**文献标识码**:A

引　言

质子交换膜燃料电池(PEMFC)具有功率密度高、工作温度低、噪声小、易于携带、启动和关闭速度快等特点,PEMFC在满足大电网难以覆盖地区家庭用电方面具有广阔应用前景。PEMFC的发电性能和使用寿命与其工作温度有密切关系[1]。质子交换膜的质子传导性和电池的功率输出将随电池温度下降而大幅下降,而过高的电池温度将导致质子交换膜脱水,严重缩短电池使用寿命。因此,必须对PEMFC的温度进行有效控制。实验结果显示,PEMFC的操作温度一般在50~110℃之间,最佳工作温度为80℃。

燃料电池是一种具有复杂电化学反应的非线性时变系统。在过去几十年里,已有较多文献基于内部机理建立了燃料电池数学建模[2~4]。这些模型适用于电池设计和性能分析,其复杂的非线性微分方程组描述的解析模型难以满足实时控制在线计算的要求。近来,递归模糊神经网络(RFNN)受到很多研究人员关注[5~6]。RFNN具有模糊系统的逻辑推理能力和神经网络在线学习能力,它的反馈连接结构也使其具有捕捉系统动态响应的功能。因此,RFNN更适于在具有非线性和时变特性的系统中应用。

本研究提出一种基于RFNN的控制器来实现PEMFC的温度控制。基于能量守恒定律建立PEMFC的动态模型;在定义RFNN控制器(RFNNC)结构的基础上,采用误差反传技术推导RFNNC参数在线更新算法;使用数值仿真验证RFNNC的有效性。

1　PEMFC热模型

单个PEMFC由双极板、气体扩散电极(由扩散层和催化层组成)和电解质膜3部分组成,PEMFC电堆由多个单个PEMFC串接而成。PEMFC使用氢气作为燃料,空气(氧气)为氧化剂。PEMFC系统一般包括3个控制子系统:温度控制子系统、压力控制子系统和功率控制子系统,如图1所示。鉴于PEMFC各被控变量(温度、压力和功率)的响应时间常数存在较大差异,温度响应速度较慢,而阴阳极气体压力和输出功率的响应速度较快,可针对各控制变量设计单独的控制回路。

燃料电池的能量损失后转换为热的形式,热以传导(conduction)的形式传播到双极板,再以对流(convection)的形式扩散到冷却水和周边空气。如果将整个电堆看作一体,在双极板中的传导现象可以忽略,认为双极板为等温体[7]。PEMFC电堆温度T_{stack}为[8]:

$$\frac{\mathrm{d}T_{stack}}{\mathrm{d}t}=\frac{1}{M_{FC}\times c_{FC}}\Big[\underbrace{Q_{loss}}_{\text{Energy loss}}+\underbrace{m_{CL}\times c_{CL}(T_1-T_2)}_{\text{Forced internal convection}}-\underbrace{k_{FC}\times(T_{stack}-T_{amb})}_{\text{Natural convection}}\Big] \tag{1}$$

收稿日期:2012 - 02 - 13;　修订日期:2012 - 03 - 12
基金项目:国家自然科学基金资助项目(61004025)

作者简介:李春华(1978 -),女,山东淄博人,江苏科技大学讲师,博士.

式中：M_{FC}—电堆质量，kg；c_{FC}—电堆的等效比热容，J/(kg·K)；Q_{loss}—能量损失；m_{CL}—冷却水流速，kg/s；c_{CL}—冷却水的等效比热容，J/(kg·K)；T_1(T_2)—冷却水进入电堆前(后)的温度，K；k_{FC}—电堆的自然对流(Natural convection)系数，W/K；T_{amb}—周边空气的温度，K。

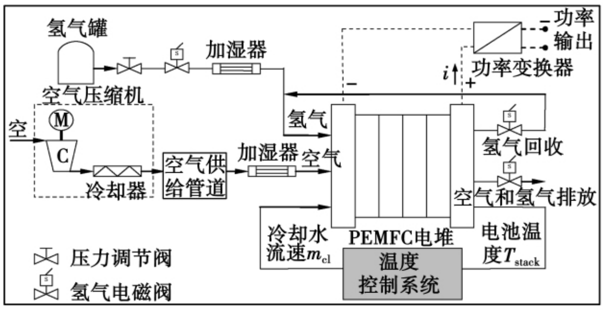

图1　燃料电池系统结构示意图

Fig. 1 Schematic diagram of the structure of a fuel cell system

电池内部的热源主要来自膜两侧催化剂层上发生电化学反应时的熵损失(Entropy loss)、氧气和H^+质子克服过电压进行传导所消耗的化学能(Overpotential loss)和水的浓缩和汽化过程中的潜热(Latent heat)[9~10]。水在汽化(evaporation)或浓缩(condensation)过程中发生的热交换Q_{phase}可以由汽化或浓缩的潜热h_{fg}和水相的变化率m_{phase}的乘积决定[10]，即：

$$Q_{phase} = m_{phase} \times h_{fg}, \begin{cases} Q_{phase} > 0 & 浓缩 \\ Q_{phase} < 0 & 汽化 \end{cases} \tag{2}$$

在燃料电池的发电过程中，水浓缩或汽化的量，和其它几种热源相比较小，在此忽略水相改变导致的热能变化量[8,11-12]。能量损失Q_{loss}为：

$$\begin{aligned} Q_{loss} &= (-\Delta H/2\mathrm{F} - V_{fc}) \times I_{fc} \\ &= \underbrace{(-\Delta H/2F - E_{Nernst}) \times I_{fc}}_{\text{Entropy loss}} \\ &\quad + \underbrace{(\eta_{act} + \eta_{ohmic} + \eta_{con}) \times I_{fc}}_{\text{Overpotential loss}} \end{aligned} \tag{3}$$

式中：ΔH—焓变，J/mol。冷却水电堆出口温度T_2由冷却水沿冷却通道得到的热能决定。这个强制性热对流(forced internal convection)过程可表示为[8]：

$$T_2 = T_{stack} - (T_{stack} - T_1)\exp\left(-\frac{A_c \times h_{FC}}{m_{CL} \times c_{CL}}\right) \tag{4}$$

式中：A_C—冷却通道的面积，cm^2；h_{FC}—内部对流系数，W/(m^2·K^1)。

2　RFNN控制器

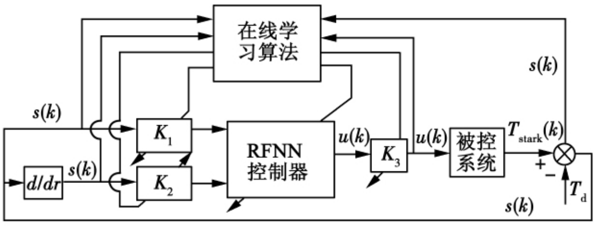

图2　基于RFNN的控制系统结构

Fig. 2 Structure of a RFNN-based control system

PEMFC电堆采用的冷却方式有风冷(小功率电堆)和水冷(中大功率电堆)两种。本研究中控制对象为2.3 kW的大电堆，需通过调节冷却水的流速来控制电堆工作温度。图2为RFNN控制器结构。控制器的输入(s，$\dot{s}$)定义为：

$$s(N) = T_{stack}(N) - T_{ref} \tag{5}$$

$$\dot{s}(N) = [e(N) - e(N-1)]/T_s \tag{6}$$

式中：T_{ref}—电池工作温度目标值；T_s—采样周期。

2.1　RFNNC结构

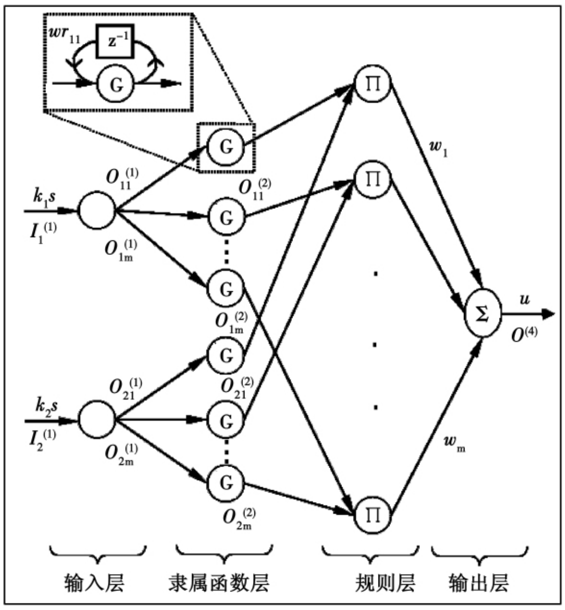

图3　RFNNC的四层网络结构

Fig. 3 Structure of a four-layer RFNNC

图3为递归模糊神经网络控制器结构，它使用一个四层网络连接结构实现模糊推理[6]。每个输入信号有m个隶属函数，RFNNC各层的输入输出

关系为:

(1) 第一层: 输入层

$$I_1^{(1)}(N) = k_1 s; I_2^{(1)}(N) = k_2 \dot{s} \tag{7}$$

$$O_{ij}^{(1)}(N) = I_i^{(1)}(N),$$
$$i = 1,2; j = 1,2,\ldots,m \tag{8}$$

式中: I—节点的输入向量; O—节点的输出向量; k_i—量化因子; N—迭代次数。

(2) 第二层: 隶属函数层

该层每个节点使用一个 Gaussian 函数作其隶属函数。第$(N-1)$次迭代信息通过递归权重 wr_{ij} 参与第 N 次迭代,即:

$$I_{ij}^{(2)}(N) = -\frac{(O_{ij}^{(1)}(N) + wr_{ij}O_{ij}^{(2)}(N-1) - a_{ij})^2}{b_{ij}^2} \tag{9}$$

$$O_{ij}^{(2)}(N) = \exp(I_{ij}^{(2)}(N)) \tag{10}$$

式中: $a_{ij}(b_{ij})$—Gaussian 函数的中心(宽度)。

(3) 第三层: 规则层

$$I_l^{(3)} = O_{1l}^{(2)} O_{2l}^{(2)}, l = 1,2,\ldots,m \tag{11}$$

$$O_l^{(3)} = I_l^{(3)} \tag{12}$$

(4) 第四层: 输出层

$$I^{(4)}(N) = \sum_{h=1}^{m} O_h^{(3)}(N) w_h,$$
$$h = 1,2,\ldots,m \tag{13}$$

$$O^{(4)}(N) = u = I^{(4)}(N) \tag{14}$$

式中: w_h—连接权重。

被控对象的控制信号为:

$$u^* = k_3 \times u \tag{15}$$

式中: k_3—比例因子。

2.2 RFNNC 参数更新

RFNNC 结构定义好后,使用基于梯度下降法的反向学习算法在线更新其参数($k_1, k_2, k_3, a_{ij}, b_{ij}, w_h, wr_{ij}$)。RFNNC 参数在线更新算法。

RFNNC 跟踪性能函数定义为:

$$E = \frac{1}{2} k_1 s^2 \tag{16}$$

第四层的误差传递项为:

$$\delta^4 = \frac{\partial E}{\partial s}\frac{\partial s}{\partial u^*} = k_1 s \frac{\partial s}{\partial u^*} \tag{17}$$

比例因子(k_3)和链接权重(w_h)的更新方法为:

$$\frac{\partial E}{\partial k_3} = \frac{\partial E}{\partial s}\frac{\partial s}{\partial u^*}\frac{\partial u^*}{\partial k_3} = \delta^4 u \tag{18}$$

$$\frac{\partial E}{\partial w_h} = \frac{\partial E}{\partial s}\frac{\partial s}{\partial u^*}\frac{\partial u^*}{\partial u}\frac{\partial u}{\partial w_h} = \delta^4 k_3 O_h^{(3)} \tag{19}$$

第三层的误差传递项为:

$$\delta_l^3 = \frac{\partial E}{\partial s}\frac{\partial s}{\partial u^*}\frac{\partial u^*}{\partial u}\frac{\partial u}{\partial O_l^{(3)}} = \delta^4 k_3 w_l. \tag{20}$$

第二层的误差传递项为:

$$\delta_{1j}^2 = \frac{\partial E}{\partial s}\frac{\partial s}{\partial u^*}\frac{\partial u^*}{\partial u}\frac{\partial u}{\partial O_j^{(3)}}\frac{\partial O_j^{(3)}}{\partial O_{1j}^{(2)}}\frac{\partial O_{1j}^{(2)}}{\partial I_{1j}^{(2)}}$$
$$= \delta_j^3 O_{2j}^{(2)} O_{1j}^{(2)} = \delta_j^3 O_j^{(3)} = \delta_{2j}^2 \tag{21}$$

隶属函数的中心(a_{ij})和宽度参数(b_{ij})的更新方法:

$$\frac{\partial E}{\partial a_{ij}} = \frac{\partial E}{\partial I_{ij}^{(2)}}\frac{\partial I_{ij}^{(2)}}{\partial a_{ij}} =$$
$$\delta_{ij}^2 \frac{2(O_{ij}^{(1)}(N) + wr_{ij}O_{ij}^{(2)}(N-1) - a_{ij})}{b_{ij}^2} \tag{22}$$

$$\frac{\partial E}{\partial b_{ij}} = \frac{\partial E}{\partial I_{ij}^{(2)}}\frac{\partial I_{ij}^{(2)}}{\partial b_{ij}} =$$
$$\delta_{ij}^2 \frac{2(O_{ij}^{(1)}(N) + wr_{ij}O_{ij}^{(2)}(N-1) - a_{ij})^2}{b_{ij}^3} \tag{23}$$

递归权重(wr_{ij})的更新方法:

$$\frac{\partial E}{\partial wr_{ij}} = \frac{\partial E}{\partial I_{ij}^{(2)}}\frac{\partial I_{ij}^{(2)}}{\partial wr_{ij}}$$
$$= \delta_{ij}^2 [2(a_{ij} - O_{ij}^{(1)}(N) -$$
$$wr_{ij}O_{ij}^{(2)}(N-1))O_{ij}^{(2)}(N-1)]/b_{ij}^2 \tag{24}$$

量化因子(k_1, k_2)的更新方法为:

$$\frac{\partial E}{\partial k_1} = \sum\nolimits_{j=1}^{m} \frac{\partial E}{\partial I_{1j}^{(2)}}\frac{\partial I_{1j}^{(2)}}{\partial O_{1j}^{(1)}}\frac{\partial O_{1j}^{(1)}}{\partial I_{1j}^{(1)}}\frac{\partial I_{1j}^{(1)}}{\partial k_1} =$$
$$\sum\nolimits_{j=1}^{m} \delta_{1j}^2 \frac{2(a_{1j} - O_{1j}^{(1)}(N) - wr_{1j}O_{1j}^{(2)}(N-1))}{b_{1j}^2} s \tag{25}$$

$$\frac{\partial E}{\partial k_2} = \sum\nolimits_{j=1}^{m} \frac{\partial E}{\partial I_{2j}^{(2)}}\frac{\partial I_{1j}^{(2)}}{\partial O_{2j}^{(1)}}\frac{\partial O_{2j}^{(1)}}{\partial I_{2j}^{(1)}}\frac{\partial I_{2j}^{(1)}}{\partial k_2} =$$
$$\sum\nolimits_{j=1}^{m} \delta_{2j}^2 \frac{2(a_{2j} - O_{2j}^{(1)}(N) - wr_{2j}O_{2j}^{(2)}(N-1))}{b_{2j}^2} \dot{s} \tag{26}$$

RFNNC 的参数学习算法为:

$$w_h(N+1) = w_h(N) - \eta_w \frac{\partial E}{\partial w_h} \tag{27}$$

$$a_{ij}(N+1) = a_{ij}(N) - \eta_a \frac{\partial E}{\partial a_{ij}} \tag{28}$$

$$b_{ij}(N+1) = b_{ij}(N) - \eta_b \frac{\partial E}{\partial b_{ij}} \tag{29}$$

$$wr_{ij}(N+1) = wr_{ij}(N) - \eta_r \frac{\partial E}{\partial wr_{ij}} \tag{30}$$

$$k_c(N+1) = k_c(N) - \eta_k \frac{\partial E}{\partial k_c}, c = 1,2,3 \tag{31}$$

式中: η_w、η_a、η_b、η_r 和 η_k—学习率(动力因子)。

3　控制仿真和性能分析

采用 PI 控制、模糊控制和 RFNNC 分别实现 PEMFC 电堆的温度控制。RFNNC 的电堆温度控制结构如图 2 所示。操作过程中，检测电堆工作温度 T_{stack}，控制器根据 T_{stack} 与温度控制目标 T_{ref}（80℃）之间的偏差 $s = T_{\text{ref}} - T_{\text{stack}}$ 调整冷却水的流速 m_{CL}。如表 1 所示，RFNNC 连接权重 w 的初始值采用了传统模糊控制的专家知识。RFNNC 其它参数初始值为：

$[a_{i1}(0), a_{i2}(0), \cdots, a_{im}(0)] = [-1, -11/12, 0, 11/12, 1]$；$b_{ij}(0) = 0.25$；$\eta_{\text{w}} = 0.1$；$\eta_{\text{a}} = \eta_{\text{b}} = \eta_{\text{r}} = \eta_{\text{k}} = 0.18$；$wr_{ij} = 0$；$m = 25$。

表 1　RFNNC 连接权重 w 的初始值

Tab. 1 Initial values of the RFNNC connecting weights w

$\dot{S}$	NB	NS	ZO	PS	PB
NB	1(w_1)	1(w_6)	2/3	1/3	0
NS	1(w_2)	2/3	1/3	0	-1/3
ZO	2/3	1/3	0	-1/3	-2/3
PS	1/3	0	-1/3	-2/3	-1(w_{24})
PB	0	-1/3	-2/3	-1	-1(w_{25})

PEMFC 电堆由 28 个有效面积为 426 cm^2 的单电池组成。PEMFC 电堆的热模型参数如表 2 所示。由于负载变化无法预测，因此将负载作为扰动量，即将跟随负载变化的电堆电流作为扰动量。电堆的电流在第 50 s 由 50A 阶跃上升为 135 A，在第 300 s 又由 135 A 阶跃下降为 75A。

表 2　PEMFC 电堆热模型参数

ab. 2 Parameters of the thermal model for the PEMFC stack

	参数值		参数值
$k_{\text{FC}}/\text{W}\cdot\text{K}^{-1}$	0.7	A_{s}/cm^2	820
$c_{\text{P,FC}}/\text{J}\cdot(\text{kg}\cdot\text{K})^{-1}$	920	M_{FC}/kg	8.8
$c_{\text{P,CL}}/\text{J}\cdot(\text{kg}\cdot\text{K})^{-1}$	4180	T_1/K	323.15
$h_{\text{FC}}/\text{W}\cdot\text{m}^{-2}\cdot\text{K}^{-1}$	3990	T_{amb}/K	298.15

图 4 为 PEMFC 电堆的冷却水流速，图 5 为 PEMFC 电堆的温度控制结果。在第 50 s 电堆电流突然增加，电堆反应生成热增加，需增大冷却水流速，才能使电堆温度不上升，并稳定在 80℃左右；在第 300 s 电堆电流突然减少，电堆反应生成热减少，需减小冷却水流速，才能使电堆温度不下降，并稳定在 80℃左右。从仿真实验结果来看，PI 控制、模糊控制和 RFNNC3 种控制方案均可将电堆工作温度稳定在设定温度。PI 控制需 150 s 达到稳态，并伴有大幅震荡；模糊控制 FLC 需 95 s 达到稳态，也伴有较大震荡。由于 PI 控制和模糊控制 FLC 的初始参数并不合适且不能在线更新，所以其收敛速度较慢，且伴有较大震荡。相比而言，具有参数在线更新能力的 RFNNC 仅需 35 s 便可达到稳态，且震荡幅度较小。

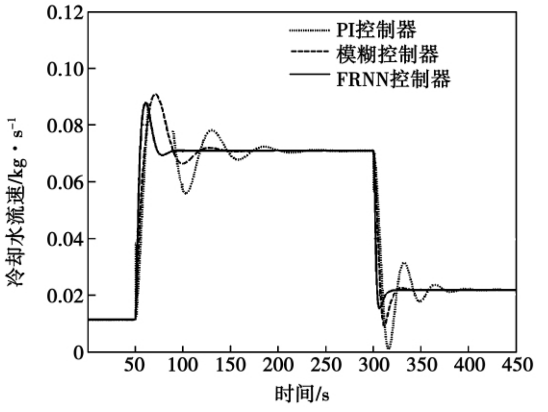

图 4　PEMFC 电堆的冷却水流速

Fig. 4 Cooling water flow speed of the PEMFC stack

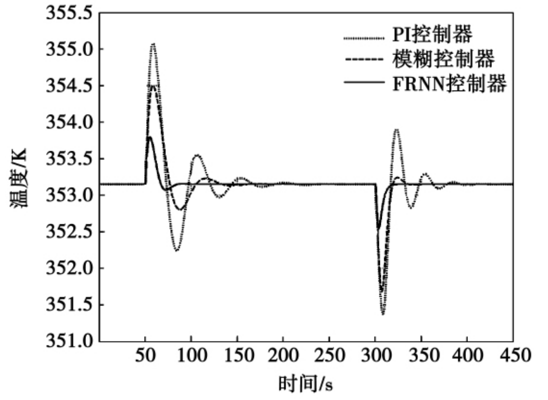

图 5　PEMFC 电堆温度控制结果

Fig. 5 Temperature control results of the PEMFC stack

4　结　论

（1）本研究推荐使用了 RFNNC 控制 PEMFC 电堆的工作温度。基于能量守恒定律建立了 PEMFC 的动态热模型；在定义 RFNNC 结构的基础上，采

用误差反传技术推导了RFNNC参数在线更新算法;使用模糊控制的专家知识对RFNNC的参数进行了初始化。

(2) 分别采用PI控制、模糊控制FLC和RFNNC实现了PEMFC电堆的温度控制。由于PI控制和FLC的初始参数不能在线更新,其收敛速度较慢,且伴有较大波动。RFNNC仅需35 s达到稳态,且波动较小,与PI和FLC的控制结果相比,RFNNC具有较好的跟踪性能。

参考文献:

[1] Coppo M,Siegel N P,Spakovsky M R V. On the influence of temperature on PEM fuel cell operation [J]. Journal of Power Sources,2006,159:560 – 569.

[2] Cheddie Dr,Munroe N. Parametric model of an intermediate temperature PEMFC [J]. Journal of Power Sources,2006,156: 414 – 423.

[3] Perng S W,Wu H W. Heat transfer in a PEMFC flow channel [J]. Applied Thermal Engineering,2009,29:3579 – 3594.

[4] Ramousse J,Deseure J,Lottin O,et al. Modeling of heat,mass and charge transfer in a PEMFC single cell [J]. Journal of Power Sources,2005,145:416 – 427.

[5] Lin F J,Huang P K,Chou W D. Recurrent – fuzzy – neural – network – controlled linear induction motor servo drive using genetic algorithms [J]. IEEE Trans Industrial Electronics,2007; 54(3): 1449 – 1461.

[6] Lin C M,Hsu C F. Supervisory recurrent fuzzy neural network control of wing rock for slender delta wings [J]. IEEE Trans Fuzzy Systems,2004; 12(5):733 – 742.

[7] Incropera F,DeWitt D. Introduction to heat transfer [M]. New York: John Wiley and Sons Press,1996.

[8] Grasser F,Rufer A. An analytical,control – oriented state space model for a PEM fuel cell system [C] //The Fourth Power Conversion Conference,Nagoya: IEEE,2007:77 – 91.

[9] Shan Y,Choe S Y. Modeling and simulation of a PEM fuel cell stack considering temperature effects [J]. J Power Source,2006,158:274 – 286.

[10] Hwang J J. A complete two – phase model of a porous cathode of a PEM fuel cell [J]. Journal of Power Sources,2007,164: 174 – 181.

[11] De Francesco M,Arato E. Start – up analysis for automotive PEM fuel cell systems [J]. J Power Sources,2000,108:41 – 52.

[12] Araki T,Koori H,Taniuchi T,et al. Simulation of the current density distribution for a PEMFC by using measured electrochemical and physical properties of the membrane [J]. J Power Sources,2005,152: 60 – 66.

(辉　编辑)

新技术、新工艺

汽轮机湿蒸汽级叶片浸蚀磨损的现状及预防措施

据《Теплоэнергетика》2011年9月刊报道,为提高汽轮机发电机组的经济性,必须解决由于提高蒸汽初参数和增加汽轮机末级叶片长度引起的一系列技术和工艺问题。

保证大功率汽轮机工作的可靠性和寿命,在很大程度上与提高运行中各种腐蚀耐受性有关,其中包括腐蚀破裂、磨蚀和水滴撞击浸蚀有关,这些都要求改进工质的质量、降低湿蒸汽级外缘的湿度、使用更完善的结构材料并研制更有效的保护涂层。

金属浸蚀研究结果的分析和结论表明了叶片材料受水滴冲击作用时表面破坏和发展的主要规律,确定所有叶片材料受液滴尺寸和表面互撞速度的影响。

提高长叶片汽轮机湿蒸汽级叶片装置耐浸蚀性最有前途的方法是表面强化并形成耐磨涂层的工艺、尽可能降低静叶和动叶栅间隙内以及根叶出汽边的湿度和大颗粒水滴的份额。

(吉桂明　摘译)

tem. Within each control periods, the error index was based to first determine whether or not it is necessary for the network to learn. If it is not necessary to learn, the PID parameters of the last control period can be used directly for control. The simulation test results obtained by using the model for main steam temperatures of thermal power plants show that the improved neural network PID control system is obviously superior to the traditional one in terms of both dynamic performance and static one. Furthermore, the training frequency of the network decreased from 7000 times before the improvement to 1732 times, lowering by more than 70%. In addition, the robustness of the improved control system has not yet been affected. **Key words:** neural network, PID (Proportional, Integral and Differential), learning, weight value, main steam temperature

竖直U型地埋管换热器热短路抑制措施的分析 = Analysis of the Measures to Prevent the Thermal Short-cut of a Vertical U-shaped Embedded Tube Heat Exchanger [刊,汉] /LIAO Quan, ZHOU Chao, CUI Wen-zhi (Education Ministry Key Laboratory on Low Quality Energy Source Utilization Technologies and Systems, College of Power Engineering, Chongqing University, Chongqing, China, Post Code: 400030) // Journal of Engineering for Thermal Energy & Power. – 2012, 27(6). –715 ~ 720

Established was a three-dimensional transient numerical model for analyzing a single U-shaped embedded tube heat exchanger and numerically simulated were various measures to prevent the "thermal short-cut" of the embedded tube heat exchanger. Under various flow carrier speeds and heat conductivity coefficients of the backfill material, the overall heat transfer performance of a heat isolation plate type and a heat isolation sleeve type embedded tube heat exchanger as well as a common embedded tube heat exchanger for which no measures was taken to prevent any thermal short-cut were studied respectively. The law governing the influence of different "thermal short-cut" prevention measures on the overall heat transfer performance of the embedded tube heat exchangers was obtained. Through a contrast analysis and comparison of the "thermal short-cut" prevention measures, which influence the overall heat transfer performance of the embedded tube heat exchangers, and in combination with the operating environment of actual embedded tube heat exchanger projects, the authors proposed that in practical engineering projects, it is not necessary to take any additional measures to prevent any thermal short-cuts of embedded tube heat exchangers. **Key words:** embedded tube heat exchanger, thermal short-cut, numerical simulation

基于递归模糊神经网络的PEMFC温度控制研究 = Study of the Temperature Control of a Proton Exchange Membrane Fuel Cell (PEMFC) Based on a Regressive Fuzzy Neural Network [刊,汉] /LI Chun-hua (Col-

lege of Electronic Information, Jiangsu University of Science and Technology, Zhenjiang, China, Post Code: 212003), ZHU Xin-jian (Fuel Cell Research Institute, Shanghai Jiaotong University, Shanghai, China, Post Code: 200240) //Journal of Engineering for Thermal Energy & Power. – 2012, 27(6). –721 ~725

The operation temperature of a proton exchange membrane fuel cell has an important influence on its power generation performance and service life. However, due to the nonlinear and time-variation characteristics of the PEMFC, it is relatively difficult for the traditional control tactics to achieve excellent temperature control performance. The authors recommended that a regressive fuzzy neural network controller (RFNNC) with a fuzzy reasoning, on-line learning and dynamic mapping ability should be used to effectively control the operation temperature of PEMFCs in an allowable range. Based on the energy conservation law, a dynamic model for PEMFCs was established. The error reverse transfer technology was employed to perform a self-adaptive adjustment of the parameters of the controller in question. The simulation test results show that the RFNNC only needs 35 seconds to attain a stable state with a relatively small fluctuation. A comparison of the control effectiveness of a RFNNC, PI control and fuzzy control indicates that the RFNNC recommended for use has a relatively good temperature tracking performance. **Key words:** proton exchange membrane fuel cell (PEMFC), thermal model, regressive fuzzy neural network (RFNN), temperature control

不同氧气浓度和粒径下工业污泥燃烧特性的实验研究 = Experimental Study of the Combustion Characteristics of Industrial Sludge at Various Oxygen Concentrations and Particle Diameters [刊, 汉] /YAN Yun-fei, ZHANG Lei, ZHANG Li, TANG Qiang (Education Ministry Key Laboratory on Low Quality Energy Source Utilization Technologies and Systems, College of Power Engineering, Chongqing University, Chongqing, China, Post Code: 400030) //Journal of Engineering for Thermal Energy & Power. – 2012, 27(6). –726 ~731

Under the condition of various oxygen concentrations and particle diameters of the sample, the thermogravimetric analytic method was used to conduct an experimental study of industrial sludge in three different industrial sectors. It has been found that the industrial sludge has good ignition and combustion characteristics and a low ignition temperature but its combustion is not intense and has low comprehensive combustion performance. To properly increase the oxygen concentration will increase the non-elementary reactions in the combustion and improve the ignition and burn-out performance of the combustion. The particle size has a big influence on the diffusion of gases and heat transfer. With a decrease of the particle diameter, the reaction interval will be narrowed and with an increase of the weight loss, the combustion weight loss rate peak value will also increase. **Key words:** industrial sludge, thermogravimetric analysis, combustion characteristics, oxygen concentration, particle diameter